# Estimating propulsive efficiency of bottlenose dolphins during steady-state swimming\*

Gabriel Antoniak<sup>1</sup>, Enric Xargay<sup>2</sup>, Joaquin Gabaldon<sup>3</sup>, Kira Barton<sup>4</sup>, Bogdan-Ioan Popa<sup>4</sup>, and K. Alex Shorter<sup>4</sup>

Abstract—Cetaceans are phenomenal swimmers, but the marine environment makes it difficult to directly observe and quantify their dynamic swimming behavior. Biologging tags are often used to measure animal movement in the wild. But these embedded systems only measure movement kinematics where they are attached, and cannot measure the hydrodynamic forces the animals use to swim. Here, we present a framework that leverages a low-order model of dolphin swimming dynamics and kinematic data (orientation, depth, speed) collected from a biologging tag to: A) estimate the sagittal-plane body kinematics of swimming bottlenose dolphins (Tursiops truncatus); and B) estimate swimming kinetics and propulsive efficiency during steady-state swimming. Body kinematics for the segmented dolphin model were estimated from tag data using a temporal convolutional network that was trained using a synthetic data set. The estimated segment angles had errors of less than  $2^{\circ}$ from the true body joint angles. The measured and estimated kinematic data were used as inputs for the dolphin model to estimate the internal and external forces generated during swimming. The estimated kinematics and kinetics compare with published results, and the estimated propulsive efficiency were typically greater than 70% across the range of swimming speeds investigated. These results enable per stoke estimates of propulsive efficiency, and provide the foundation for an approach that can be used in the future to estimate the swimming biomechanics of dolphins in the wild.

# I. INTRODUCTION

Cetaceans, an order containing porpoises, dolphins, and whales, are highly efficient swimmers, with estimated swimming efficiencies exceeding 70% [1]–[4]. Estimates of hydrodynamic forces are key to investigating swimming biomechanics, thrust production, and efficiency. Simple hydromechanical models have been used to estimate both the drag acting on the animal [5], [6], and propulsive forces generated by the fluke moving through the water [2], [7], [8]. These simple, computationally efficient models usually involve limiting assumptions of inviscid flows or very small amplitudes of oscillation. Additionally, these approaches

estimate propulsive force indirectly by modeling the drag force created by the animals body as it moves through the water, abstracting away the movement of the dolphin body during swimming. On the other end of the spectrum, computational fluid dynamics (CFD) simulations of dolphin swimming have also been performed [1], [9], [10] to estimate the kinetics and efficiency of dolphin swimming, but require extensive computational time due to the model complexity. Further, even these CFD simulations typically disregard the flexibility of the dolphin fluke.

Both the simple and complex modeling approaches require information about animal kinematics. The simple models use measurements of speed, acceleration, orientation and depth to estimate propulsive forces [11]. CFD simulations require fluke kinematics (amplitude, frequency, angle of attack), body morphology, and the full animal pose during the stroke cycle. The underwater environment makes capturing such kinematics challenging, typically requiring the use of an underwater camera and clear water for good visibility [12], [13]. However, a camera based approach can only record a few consecutive stroke cycles while the dolphin is in the frame. In place of measured kinematics, CFD simulations often assume the body motion, as in [1], or scale and apply the body kinematics of different cetacean species whose kinematics were better studied, as in [9], where the swimming kinematics of an orca were combined with a dolphin swimming model.

Biologging tags use a combination of sensors, such as inertial measurement units (IMUs), pressure sensors, and speed sensors, to continuously measure swimming kinematics (depth, acceleration, speed, angular velocity, and heading) [14], [15]. These sensors are also used to estimate body pose (pitch, roll). Most studies of wild cetacean populations use only a single tag on the animal to parameterize whole body kinematics [15]-[17]. In humans, data from multiple kinematic sensors have been combined with filtering approaches to estimate whole body kinematics during walking [18], [19]. But these approaches are challenging to replicate with cetaceans, as increased drag loading from tags can influence dolphin swimming kinematics [15], meaning that multiple-tag setups may not necessarily capture biological swimming gait depending on the tag size and their associated drag. The work in [20] used data from a single IMU on the lower back to infer the body joint angles of both legs during human walking, but this type of approach has not been applied to data from cetaceans. Directly estimating the full

<sup>\*</sup>The work was partially supported by a Contribution Agreement with the Department of Fisheries and Oceans Canada (DFO), and the National Science Foundation under Grant No. 2238432.

<sup>&</sup>lt;sup>1</sup> Gabriel Antoniak is a PhD Candidate in the Department of Mechanical Engineering, at the University of Michigan, Ann Arbor; e-mail: gjantoni@umich.edu

<sup>&</sup>lt;sup>2</sup> Enric Xargay was a visiting scholar at the Department Mechanical Engineering at the University of Michigan, Ann Arbor.

<sup>&</sup>lt;sup>3</sup> Joaquin Gabaldon was a postdoctoral researcher in the Department of Mechanical Engineering at the University of Michigan, Ann Arbor.

<sup>&</sup>lt;sup>4</sup> Kira Barton, Bogdan-Ioan Popa, and K. Alex Shorter are faculty members in the Department of Mechanical Engineering at the University of Michigan, Ann Arbor.

body kinematics from the hydromechanical model in [21] is not feasible: the model assumes dolphin-like swimming body motion based on an "average" dolphin, with swimming gait enforced by controllers. However, real-world swimming exhibits varying torso and body kinematics that are not the "average", and thus using the assumed body motion does not reflect each individual's swimming gait. Furthermore, this assumed "average" dolphin profile is based on a limited amount of kinematic data, due to the challenges in collecting such data. The work in [22] has shown that there exist correlations in the phasing and amplitude of oscillation of different points on the cetacean body, which makes a data science approach especially amenable to extracting that information from a single-point proxy.

Data science approaches have been used to infer the mapping from IMU measurements to body joint angles in human walking with data from single or multiple IMU systems using densely connected networks [20], [23], generalized regression networks [24], or long short-term memory (LSTM) networks [23]. These approaches correct for sensor bias and drift before inputting the accelerations, angular rates, and orientation into a neural network. Using the temporal nature of the data collected during cyclic movement has also been shown to improve predictions [23]. However, most methods tend to treat each data point individually, neglecting important temporal information [20]. These approaches can allow for individual-specific estimates of body posture during gait, rather than predictions of average motion. To address these gaps in cetacean swimming, we propose a framework for estimating the kinetics and propulsive efficiency of swimming bottlenose dolphins using a single kinematic tag with a low-order model of dolphin swimming dynamics. This framework is then used to characterize the propulsive efficiency of dolphins during steady-state swimming.

## II. METHODS

## A. Modeled dolphin swimming kinematics and kinetics

This work leverages a physics-based, low-order model of the swimming dynamics of a bottlenose dolphin, which captures critical features such as body posture, fluke flexibility, and delayed fluke stalls [21]. The modeling framework is based on a mixed Newtonian-Lagrangian formulation. The head, torso, caudal peduncle, and pectoral fins are modeled as interconnected rigid bodies, whereas the fluke is modeled as a flexible plate, whose transverse deformation evolves in response to the fluke's hydrodynamic, elastic, and inertial forces. Because hydrodynamic loading over the fluke is in turn affected by its deformation state, the model incorporates existing results from unsteady lifting-line theory to predict lift, drag, and pitching-moment distributions over the deforming fluke. The configuration of the body segments during swimming are defined by three joint angles: the headtorso angle  $(\theta_H)$ , the torso-peduncle 1 angle  $(\theta_{P1})$ , and the peduncle 1-peduncle 2 angle  $(\theta_{P2})$ . The joint between the peduncle and the fluke is assumed to be a semi-passive joint with nonlinear stiffness. Feedback control was used with the model to track a desired speed input by modulating the

frequency and amplitude of the joint angles. Kinematic data (joint angles, angular rates, and center of mass swimming speed) from these simulations were used to create a synthetic data set to train the neural network presented in this work, Figure 1.

The hydromechanical model was used to simulate swimming kinematics at speeds ranging from 0.6 to 2.3 body lengths per second (BL/s) in increments of 0.1 BL/s for 30-second steady-state swimming bouts. This speed range covers the typical range of sustainable swimming speeds for bottlenose dolphins. From these 30-second segment increments, shorter 3 second segments were randomly sampled from the longer period and used for generating the training samples. For each short segment, Gaussian noise was added to the horizontal speed and torso attitude during training to further augment the data. An example of the inputs and outputs of the model used for data generation is presented in Figure 1.

## B. Neural network architecture

The temporal nature of the sequence of body kinematics during steady-state swimming was leveraged to improve the accuracy of whole-body kinematics estimates. Temporal convolution networks (TCNs) are well-suited for mapping sequences to sequences. These networks are built by layers of increasingly dilated convolutions [25]. Like LSTMs, TCNs can handle sequences of arbitrary length. However, TCNs converge to solutions faster than LSTMs, and these solutions tend to be more accurate than those of LSTMs [25]. As such, the TCN architecture was selected to learn the mapping from the torso kinematics and speed to the whole-body kinematics.

Half of the speeds from the synthetic data set were used for training, a quarter for validation to check model performance during training, and the last quarter for testing the trained network on data it has not seen before. The model was trained for 2500 epochs, with adaptive moment estimation (ADAM) as the optimizer. The network weights at the end of each epoch that best performed on the validation set were saved. The network hyperparameters in this study were a kernel size of 3, channel sizes of 64, 32, 16, 8, 3 for the layers, and a dilation factor of 2.

# C. Biologging tag data

Biologging tags were used to collected movement data from bottlenose dolphins during prescribed straight-line swimming tasks. A tag was placed on the animals' torso between the dorsal fin and the blow hole using 4 suction cups. Measurements of acceleration, angular velocity, heading, depth, and speed were collected during the swimming trials. Data collection was conducted in a shallow water lagoon environment at Dolphin Quest Oahu. During the trials the animals swam across the lagoon and back ( $\approx 80$  m) over a range of self selected speeds. Tag data were processed as in [11], [14], [15] to correct for bias and drift in the IMU measurements, as well as correcting the depth based on the speed and the orientation of the animal. Six animals

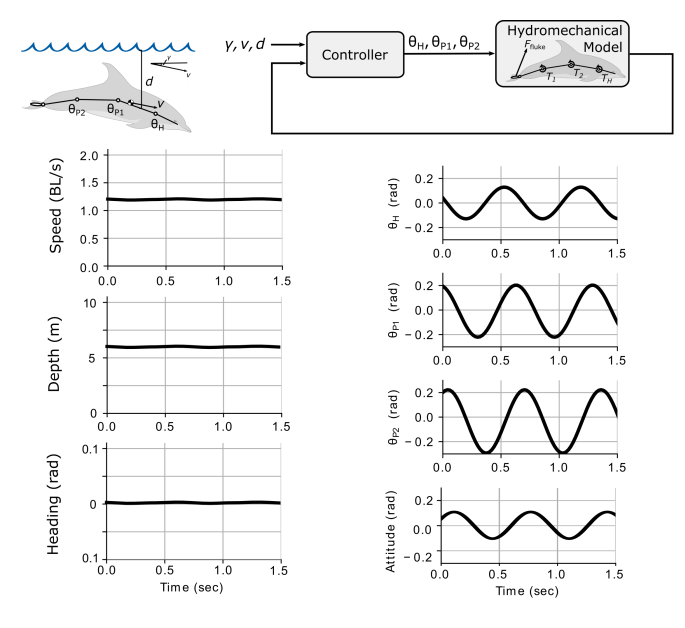


Fig. 1. Example of how the synthetic data was generated. Speed v, depth d, and heading  $\gamma$  were specified for the hydromechanical model. Feedback was used to control the movement of the body joints  $(\theta_H, \theta_{P1}, \text{ and } \theta_{P2})$  to track the input speed, depth, and heading. Note that the system can well-track these parameters, and thus they vary little with time. Once the system reached steady-state, the three body joint angles were extracted, as well as the attitude of the torso. The speed and attitude of the torso were used as inputs to the neural network, and the three body joint angles as outputs for the model

participated in the trials, with 195 identified bouts of steady-state swimming that were used for the analysis presented here. Animals ranged in length from 2.19 m to 2.54 m from rostrum to the fluke's insertion onto the caudal peduncle, and varied in mass from 143 kg to 245 kg (see Table II). Flukes were imaged and traced for their leading and trailing edges, and their span measured. For the purposes of the sagittal-plane model used [21], the left half of the fluke was mirrored to the right half to ensure bilateral symmetry. The self-selected swimming speed of the dolphins during the lap trials ranged from 2.24 m/s to 5.41 m/s.

TABLE I
PARAMETERS OF DOLPHINS STUDIED

Dolj	phin	Mass [kg]	Length [m]	Fluke Span [cm]
	Ĺ	185.7	2.48	58.7
2	2	142.6	2.35	59.8
5	3	208.8	2.51	76.4
4	1	156.2	2.36	56.4
	5	244.7	2.71	73.9
(	5	185.7	2.39	69.7
$-\mu$	±σ 18	$37.3 \pm 36.7$	$2.32 \pm 0.12$	$65.8 \pm 8.6$

## D. Estimating swimming kinetics for tag data

Figure 2 presents the framework used to estimate swimming kinetics from tag measurements. In this approach, the IMU data from the tag data was first filtered and used to estimate the instantaneous speed and torso attitude. These

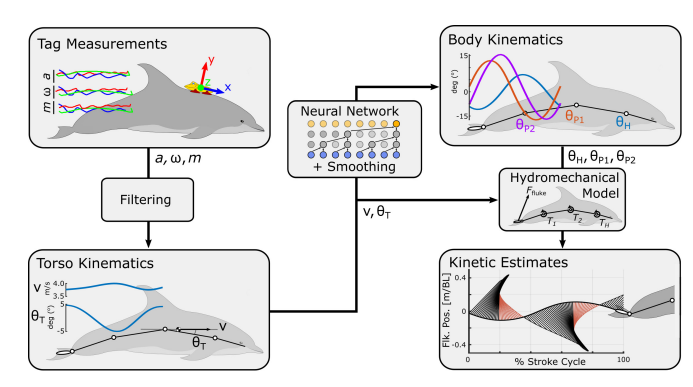


Fig. 2. The proposed framework for estimating kinetics and efficiency of cetacean swimming. First, a biologging tag anterior to the dorsal fin makes measurements of the speed, linear accelerations a, gyro rates  $\omega$ , and orientation m. These are filtered to yield the torso attitude and the instantaneous speed. These filtered data are fed into a neural network to estimate body kinematics. Finally, the filtered data and the output of the neural network are used as inputs to the hydromechanical model to yield estimates of thrust power, as well as the internal joint powers, from which efficiency can be calculated.

parameters were then used as inputs for the trained neural network.

Outputs from the network (the head-torso ( $\theta_H$ ) angle, the torso-peduncle 1 ( $\theta_{P1}$ ) angle, and the peduncle 1-peduncle  $2 (\theta_{P2})$  angle) were smoothed forwards and backwards with a 3rd-order Butterworth filter with a cutoff frequency of 5 Hz, similar to the work of [26]. The predictions of body kinematics, along with the speed and torso attitude, were next used to prescribe the instantaneous pose of the dolphin for the simulations using the hydromechanical model. At the start of the simulation, the angle and angular rate of the passive Fluke-Peduncle 2 joint were assumed to be zero. To account for these arbitrary initial conditions, the first stroke cycle in a bout of steady state swimming was looped 30 times to create an approximately 30 second window for the model to reach a steady state before the kinetics of the swimming bout were simulated. An example of the estimated force generated by the fluke during a cycle is shown in the lower right of the Figure 2. During each stroke cycle, there are regions where the force generated by the fluke produces thrust (horizontal component is in the direction of travel, force vectors in black in the figure), and where the hydrodynamic force produces drag (red force vectors in the figure). These regions of drag occur at the transitions between upstrokes and down strokes. An inverse dynamics approach was then used with the estimated kinematics and kinetics to estimate the internal torques at the model joints. Propulsive efficiency for each steady-state fluking bout,  $\eta$ , was calculated as the ratio of the mean thrust power (the average thrust force,  $\overline{T}$  multiplied by the mean horizontal speed, U) to the mean power generated by peduncle segments to move the fluke  $(\overline{P})$  over the fluking bout:

$$\eta = \frac{\overline{T}U}{\overline{P}} \tag{1}$$

#### III. RESULTS

#### A. Neural network

The trained network performed well with the test data from the synthetic data set. Results for the three body joint angles are summarized in Table I. On average, the  $\theta_H$  joint angle had the lowest error, followed by the  $\theta_{P1}$  angle, with the  $\theta_{P2}$  angle having the highest error. Overall the errors in the angles were low, with an average root-mean-squared error (RMSE) of less than  $1^\circ$  for each of the joint angles in the 3 second swimming bouts. There is high correlation between the joint angles predicted by the network and the true joint angles from the simulated data, with the correlation exceeding 0.99 for all three joint angles. On average, about 97% of the angles predicted for the three body joint angles were within  $2^\circ$  of the true angle.

TABLE II

QUANTITATIVE PERFORMANCE OF NETWORK ON THE 3 SECOND SEGMENTS OF SIMULATED STEADY STATE SWIMMING.

Body Joint	$\theta_H$	$ heta_{P1}$	$\theta_{P2}$
RMSE (°)	$0.32 \pm 0.37$	$0.60 \pm 0.66$	$0.72 \pm 0.76$
Within 1°(%)	$97.8 \pm 5.6$	$90.9 \pm 13.2$	$86.8 \pm 17.1$
Within 2°(%)	$99.9 \pm 0.2$	$98.7 \pm 3.4$	$97.7 \pm 4.8$
Correlation	$0.998 \pm 0.002$	$0.997\pm0.003$	$0.997\pm0.003$

# B. Estimating swimming kinematics and kinetics

The fluke cycle frequency and the normalized speed (mean speed normalized by dolphin body length) are within the range presented in the literature [12] (see Figure 3A). The work in [12] shows a larger increase in frequency than what we observed in the swimming dolphins. Data in [12] were generated by manually analyzing video frames. Peak-to-peak amplitude of the trailing edge of the fluke was also calculated for the swimming bouts (Figure 3B). The predicted fluking amplitude is on average greater than that found in [12]. However, when looking at the Strouhal number, a nondimensional parameter that relates fluking frequency f, amplitude L, and mean speed U (fL/U), the model's predictions are within the range seen in [22]. As speed increased, the thrust power at the fluke was predicted to increase. Estimated thrust power was comparable with previous literature (Figure 3D). The internal joint powers are plotted in Figure 4A while the efficiencies —the ratio between thrust power and internal joint power— are plotted in Figure 4B.

# IV. DISCUSSION

This work presents novel estimates of propulsive efficiency derived from data collected with a biologging tag. These results offer new insight into dolphin biomechanics and are an important first step towards the investigation of swimming kinetics in wild dolphins. Measured speed (impeller) and orientation (IMU) during steady state swimming were used with a neural network to estimate body kinematics. A model was used to generate the body kinematics to train the network because we lacked measured whole body kinematics that spanned the range of observed swimming speeds during

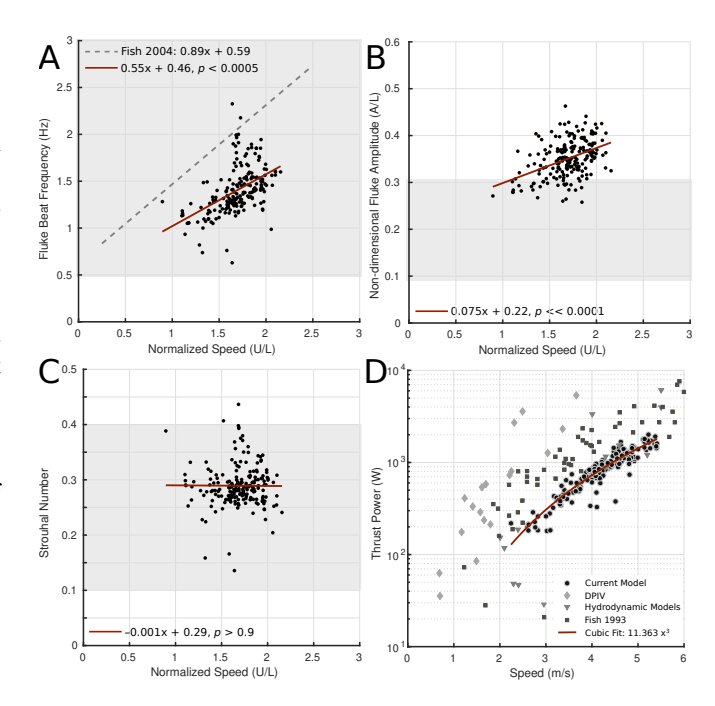


Fig. 3. Comparison of model output and predictions with current literature. A Dolphin fluking frequency versus normalized speed (velocity normalized by body length). Shading indicates the region of dolphin fluking frequencies in literature, with the dashed regression line taken from [12] as the best fit line to their data. Solid red line represents line of best fit for our data points (black circles). B Fluking amplitude normalized by the body length versus the normalized speed. The neural network predictions coupled with hydromechanical model result in trailing edge fluking amplitude being slightly greater than the range previously published in [12] (shaded region). C The Strouhal number versus normalized speed. The line of best fit is horizontal, and almost every single dolphin swimming bout is within the ideal 0.2-0.4 range published in [27], while almost every point resides in the range seen in [12] (shaded region). D The thrust power versus speed for our model (black circles) in comparison to other models and experimental predictions: digital particle image velocimetry (DPIV) experiments [13] as diamonds, other hydrodynamic models as triangles, and other estimates published in [28] as squares. The solid red line represents the best fit of a cubic term.

experimental data collection. Output from the neural network (segment angles) and filtered IMU data and speed measurements were used an inputs for a physics-based model of dolphin swimming to yield predictions of the hydrodynamic forces generated by the fluke and the internal torques at the modeled joints. Estimates of fluking frequency and amplitude of the fluke during a cycle were compared to measured kinematics from the literature. Though our estimated fluking amplitude is larger than that found in literature, the resulting Strouhal numbers fall within the ideal range of 0.2 to 0.4. This range of Strouhal numbers is a feature present across different types of biological locomotion, from the swimming of dolphins [12], to the swimming of sharks and bony fish, as well as the flight of birds, bats, and insects during steady-state motion [27].

As can be seen in Figure 3, results from the framework compare well to other hydrodynamic models and digital particle image velocimetry (DPIV) estimates of thrust power. Direct comparisons were made more difficult because results in the literature were not normalized for animal size, but

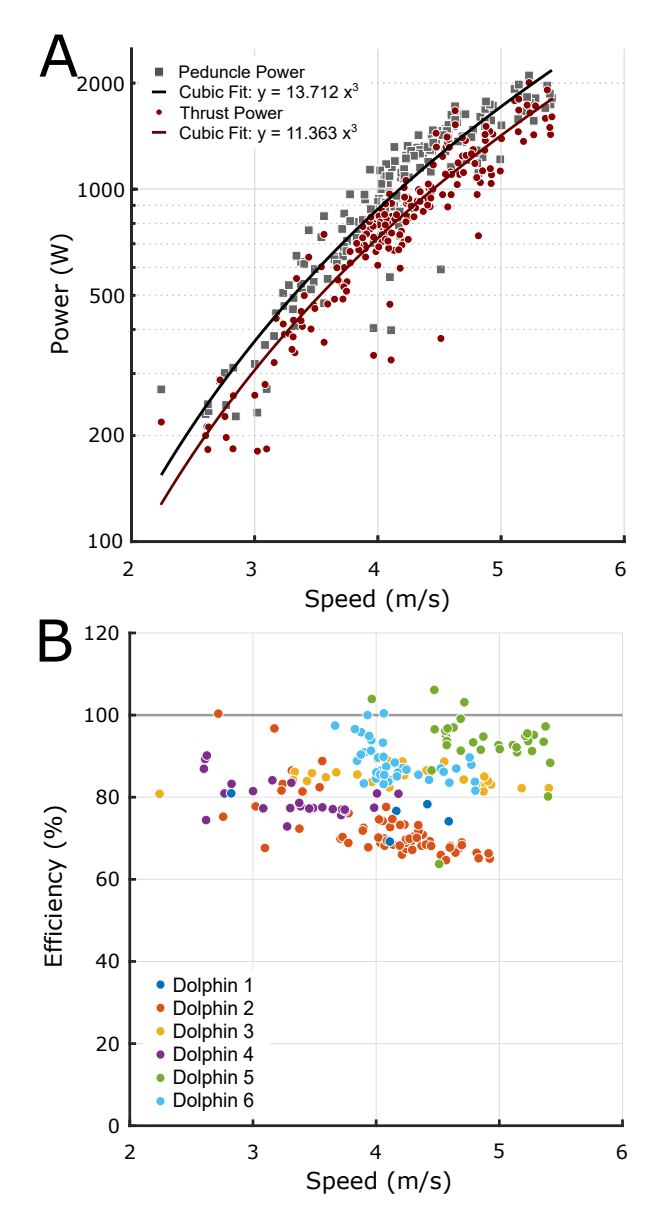


Fig. 4. Internal joint power and swimming efficiency. A Internal joint power (black) is compared with the external thrust power (red). The internal joint power increases with an increase in speed (regression curve, solid black), and exceeds the thrust power (regression curve, red). B The efficiency of each swimming stroke cycle, that is, the ratio of the thrust power to the internal joint power for each individual fluking bout. Each color represents a specific dolphin, and each point represents a steady-state swimming bout.

differences between the presented results and the literature could be due to model parameter selection. The model in this work uses animal-specific parameters, namely the mass and length, and assumes a fineness ratio (ratio of length and width) for the body of the animal to account for some difference in body shapes. However, the dorsal and pectoral fins shape were assumed and scaled between animals with regards to size. Only the fluke parameters were based on images taken of individual dolphin flukes. Thus, the accuracy of the model's input parameters could be further improved by using more animal specific parameters.

With the proposed framework, we were able to make

predictions of the propulsive efficiency of swimming. There have been comparatively few studies that look at the phased motion of dolphin swimming; the work in [3] is one such example. More studies have been done on fish [29], because the small size of fish enables the study of swimming dynamics in controlled experimental environments. With regards to propulsive efficiency, the current framework enables individual predictions for each of the dolphins that participated in the work. The efficiencies tend to exceed 70%, and all exceed 56% efficiency reported by [9]. Though that study involved a CFD simulation of a swimming porpoise scaled up to the size of an orca due to the availability of good kinematic data of orca swimming (and the lack of available porpoise body kinematics during swimming). These results demonstrate the promise this approach has for estimating these difficult-tomeasure quantities.

This method leverages the phased nature of dolphin swimming and data from bio-logging tags, enabling estimates of motion and forces during free swimming. This greatly expanded context for kinetic estimates mitigates the difficulty of observing animal behavior underwater, a medium with poor visibility, difficulty observing with sensors, and very large areas that would have to covered for studying wild populations. In the future, combining this approach with measurements of animal physiology would provide further insight into dolphin biomechanics. For example, measurements of blood oxygenation during swimming could be used to improve cost estimates in future work [30]. Adding electromyography (EMG) to the tag measurements would enable the investigation of muscle activation during swimming. These indirect measurements would inform model predictions, considering that directly measuring the outputs of the model —forces produced by the fluke during swimming, or the powers generated internally by the dolphin to drive the fluke— cannot be directly measured otherwise.

These results are promising, but this approach requires further validation with real-world dolphin swimming. Comparing the mechanical cost of swimming estimated using this approach with estimates of metabolic cost using respirometry would be an important next step [11], [15]. These studies typically assume about a 25% efficiency for generating muscle power from metabolic processes [11]. We have shown that the neural network approach results in dolphin-like kinematics predictions using real-world data, which when input into the hydromechanical model yield realistic estimates of the kinetics and efficiency, but quantifying the error in predicted body kinematics should be investigated. The trained network gives excellent predictions on the synthetic data set, with errors ranging from about 1-2% of the peak-to-peak amplitude of oscillation, and with high correlation between the predicted joint angles and the true joint angles. However, acquiring more experimentally collected kinematic data will allow us to better quantify the estimated errors that can result from this method and properly validate its predictive power on individual-specific swimming gait profiles. This discrepancy in body motion could be one cause of the swimming bouts that had predicted efficiencies exceeding 100%. Another source of this discrepancy could be internal to the model itself: some of the fluke hydrodynamics are estimated or assumed based on hydrofoil literature, and might not necessarily reflect the true, but uncertain, properties of dolphin flukes.

## **ACKNOWLEDGMENT**

G.A. and K.A.S. would like to thank Frank Fish for the discussions pertaining to dolphin swimming: Strouhal number, fluke deformations, and fluke stiffness. Additionally, we would like to thank everyone at Dolphin Quest Oahu for their help in running the experiments.

#### REFERENCES

- [1] X. Wang, P. Wei, Y. Yuan, Z. Zhang, and D. Feng, "Evaluation of dolphin swimming speed and thrust based on CFD," *International Journal of Offshore and Polar Engineering*, vol. 28, no. 2, pp. 120– 127, 2018.
- [2] N. Bose and J. Lien, "Propulsion of a Fin Whale (Balaenoptera physalus): Why the Fin Whale is a Fast Swimmer," *Proceedings of* the Royal Society of London. Series B, Biological Sciences, vol. 237, no. 1287, pp. 175–200, 1989.
- [3] F. E. Fish and C. A. Hui, "Dolphin swimming-a review," *Mammal Review*, vol. 21, no. 4, pp. 181–195, 1991.
- [4] F. E. Fish, "Limits of Nature and Advances of Technology: What Does Biomimetics Have to Offer to Aquatic Robots?" *Applied Bionics and Biomechanics*, vol. 3, no. 1, pp. 49–60, 2006.
- [5] J. Gray, "Studies in Animal Locomotion: VI. The Propulsive Powers of the Dolphin," *Journal of Experimental Biology*, vol. 13, no. 2, pp. 192–199, 1936.
- [6] K. A. Kermack, "The Propulsive Powers of Blue and Fin Whales," Journal of Experimental Biology, vol. 25, no. 3, pp. 237–240, 1948.
- [7] M. J. Lighthill, "Aquatic animal propulsion of high hydromechanical efficiency," *Journal of Fluid Mechanics*, vol. 44, no. 2, pp. 265–301, 1970
- [8] M. Chopra and T. Kambes, "Hydromechanics of lunate-tail swimming propulsion . Part 2," *Journal of Fluid Mechanics*, vol. 79, pp. 49–69, 1077
- [9] A. von Loebbecke, R. Mittal, F. Fish, and R. Mark, "Propulsive efficiency of the underwater dolphin kick in humans," *Journal of Biomechanical Engineering*, vol. 131, no. 5, pp. 1–4, 2009.
- [10] R. C. Z. Cohen and P. W. Cleary, "Computational studies of the locomotion of dolphins and sharks using smoothed particle hydrodynamics," *IFMBE Proceedings*, vol. 31, pp. 22–25, 2010.
- [11] J. T. Gabaldon, D. Zhang, J. Rocho-Levine, M. J. Moore, J. van der Hoop, K. Barton, and K. A. Shorter, "Tag-based estimates of bottlenose dolphin swimming behavior and energetics," *Journal of Ex*perimental Biology, vol. 225, no. 22, 2022.
- [12] J. J. Rohr and F. E. Fish, "Strouhal numbers and optimization of swimming by odontocete cetaceans," *Journal of Experimental Biology*, vol. 207, no. 10, pp. 1633–1642, 2004.
- [13] F. E. Fish, P. Legac, T. M. Williams, and T. Wei, "Measurement of hydrodynamic force generation by swimming dolphins using bubble DPIV," *Journal of Experimental Biology*, vol. 217, no. 2, pp. 252–260, 2014.
- [14] K. Alex Shorter, Y. Shao, L. Ojeda, K. Barton, J. Rocho-Levine, J. van der Hoop, and M. Moore, "A day in the life of a dolphin: Using bio-logging tags for improved animal health and well-being," *Marine Mammal Science*, vol. 33, no. 3, pp. 785–802, 2017.
- [15] J. M. van der Hoop, A. Fahlman, K. A. Shorter, J. Gabaldon, J. Rocho-Levine, V. Petrov, and M. J. Moore, "Swimming energy economy in bottlenose dolphins under variable drag loading," *Frontiers in Marine Science*, vol. 5, no. DEC, pp. 1–13, 2018.
- [16] J. W. Durban and R. L. Pitman, "Antarctic killer whales make rapid, round-trip movements to subtropical waters: Evidence for physiological maintenance migrations?" *Biology Letters*, vol. 8, no. 2, pp. 274– 277, 2012.
- [17] G. S. Schorr, E. A. Falcone, D. J. Moretti, and R. D. Andrews, "First long-term behavioral records from Cuvier's beaked whales (Ziphius cavirostris) reveal record-breaking dives," *PLoS ONE*, vol. 9, no. 3, 2014.

- [18] M. V. Potter, S. M. Cain, L. V. Ojeda, R. D. Gurchiek, R. S. McGinnis, and N. C. Perkins, "Error-state Kalman filter for lower-limb kinematic estimation: Evaluation on a 3-body model," *PLoS ONE*, vol. 16, no. 4 April, pp. 1–21, 2021. [Online]. Available: http://dx.doi.org/10.1371/journal.pone.0249577
- [19] T. McGrath and L. Stirling, "Body-worn imu human skeletal pose estimation using a factor graph-based optimization framework," *Sensors (Switzerland)*, vol. 20, no. 23, pp. 1–29, 2020.
- [20] H. Lim, B. Kim, and S. Park, "Prediction of lower limb kinetics and kinematics during walking by a single IMU on the lower back using machine learning," Sensors (Switzerland), vol. 20, no. 1, 2020.
- [21] E. Xargay, K. Barton, G. Antoniak, and K. A. Shorter, "A Low-Order Model of Dolphin Swimming Dynamics: Fluke Flexibility and Energetics," *CCTA* 2023 Submission, 2023.
- [22] F. E. Fish, J. E. Peacock, and J. J. Rohr, "Stabilization mechanism in swimming odontocete cetaceans by phased movements," *Marine Mammal Science*, vol. 19, no. 3, pp. 515–528, 2003.
- [23] M. Mundt, W. Thomsen, T. Witter, A. Koeppe, S. David, F. Bamer, W. Potthast, and B. Markert, "Prediction of lower limb joint angles and moments during gait using artificial neural networks," *Medical and Biological Engineering and Computing*, vol. 58, no. 1, pp. 211–225, 2020
- [24] A. Findlow, J. Y. Goulermas, C. Nester, D. Howard, and L. P. Kenney, "Predicting lower limb joint kinematics using wearable motion sensors," *Gait and Posture*, vol. 28, no. 1, pp. 120–126, 2008.
- [25] S. Bai, J. Z. Kolter, and V. Koltun, "An Empirical Evaluation of Generic Convolutional and Recurrent Networks for Sequence Modeling," arXiv, 2018. [Online]. Available: http://arxiv.org/abs/1803.01271
- [26] M. Mundt, A. Koeppe, S. David, T. Witter, F. Bamer, W. Potthast, and B. Markert, "Estimation of Gait Mechanics Based on Simulated and Measured IMU Data Using an Artificial Neural Network," Frontiers in Bioengineering and Biotechnology, vol. 8, no. February, pp. 1–16, 2020.
- [27] G. K. Taylor, R. L. Nudds, and A. L. Thomas, "Flying and swimming animals cruise at Strouhal number tuned for high power efficiency," *Nature*, vol. 425, pp. 707–710, October 2003.
- [28] F. E. Fish, "Power output and propulsive efficiency of swimming bottlenose dolphins (Tursiops truncatus)," *Journal of Experimental Biology*, vol. 185, pp. 179–193, 1993.
- [29] J. Zhu, C. White, D. K. Wainwright, V. DiSanto, G. V. Lauder, and H. Bart-Smith, "Tuna robotics: A high-frequency experimental platform exploring the performance space of swimming fishes," *Science Robotics*, vol. 4, 2019.
- [30] T. Hamaoka and K. K. McCully, "Review of early development of near-infrared spectroscopy and recent advancement of studies on muscle oxygenation and oxidative metabolism," *The Journal of Physiological Sciences*, vol. 69, pp. 799–811, 2019.